

## TAKING INTO ACCOUNT UNCERTAINTIES TO ANALYZE THE ROBUSTNESS OF AN ENERGY PUMPING SYSTEM

**Edson Cataldo<sup>a</sup>, Sergio Bellizzi<sup>b</sup> and Rubens Sampaio<sup>c</sup>**

<sup>a</sup>*Applied Mathematics Department, Graduate Program in Telecommunications Engineering,  
Universidade Federal Fluminense, Rua Mário Santos Braga, S/N, Centro, Niteroi, RJ, CEP:24020-140,  
Brazil, ecataldo@im.uff.br*

<sup>b</sup>*Laboratoire de Mécanique et d'Acoustique, CNRS, 31 chemin Joseph Aiguier, 13402 Marseille,  
France, bellizzi@lma.cnrs-mrs.fr*

<sup>c</sup>*Mechanical Engineering Department, PUC-Rio, Rua Marquês de São Vicente, 225 Rio de Janeiro, RJ,  
CEP: 22453-900, Brazil, rsampaio@puc-rio.br*

**Keywords:** energy pumping, energy transfer, passive control, uncertainties.

### **Abstract.**

Energy pumping is defined as the irreversible energy transfer from one structure (linear and the so-called primary structure) to another structure (essentially nonlinear and the so-called non-linear energy sink (NES)) which is coupled with the primary structure. The principle of energy pumping has been analyzed theoretically and also validated experimentally. The aim of this paper is to study the energy pumping robustness considering the uncertainties of the parameters of a two DOF mass-spring-damper system composed of two subsystems: one linear subsystem, the primary structure, and one nonlinear subsystem, the NES. The two subsystems are coupled by a linear spring and the whole system corresponds to a grounded configuration. Three parameters of the system will be considered as uncertain: the coupling linear spring, the damper from the nonlinear system and the damper from the linear subsystem. Probability density functions are constructed for the random variables associated to the uncertain parameters applying the Maximum Entropy Principle. A sensitivity analysis is then performed. Depending on the dispersion, the pumping energy can be highly influenced.

## 1 INTRODUCTION

Targeted Energy Transfer (TET) refers to a mechanism where energy is transferred in a one-way irreversible fashion from a source to a receiver. TET occurs in a wide range of both physical phenomena and engineering applications. In the context of passive vibration control of mechanical systems, TET has been used to develop a new concept of nonlinear dynamic absorber. In this case, the irreversible energy transfer, also named energy pumping, occurs from the main or primary structure, which needs to be protected, to the nonlinear absorber coupled with the first one. The nonlinear absorber also named Nonlinear Energy Sink (NES) consists of a mass with an essentially nonlinear spring. This concept involves nonlinear energy interactions which occur due to internal resonances making possible irreversible nonlinear energy transfers from the primary system to the attachment. The nonlinear energy pumping was first described in (Gendelman et al., 2001; Vakakis and Gendelman, 2001). Comparing the NES with the corresponding linear dynamic absorber (also known as Frahm absorber or Helmholtz resonator), some interesting characteristics can be highlighted. The nonlinear absorbers operate in a large frequency band and not only with frequencies near the natural frequency of the primary system. Since the NES is essentially nonlinear, these systems have no natural frequencies and they are effective for a large range of frequencies, while the linear absorbers attenuate only one frequency with good accuracy. A complete description of the TET can be found in (Vakakis et al., 2008).

In parallel to theoretical and numerical studies, the concept of NES has also been developed and validated experimentally. In the context of vibration reduction, essential stiffness nonlinearities (which cannot be linearized) have been experimentally implemented considering two springs such that a polynomial nonlinearity (in general cubic) can be obtained. In (Jang et al., 2003), piano wires were used as springs whereas in (Gourdon et al., 2007) two linear helical springs were considered. Essential stiffness nonlinearity has also been experimentally implemented using a single mass in a vibroimpact system (Nucera et al., 2008). Note that the vibroimpact NES can be viewed as a generalization of the passive impact damper studied in (Ema and Marui, 1994) where the efficiency was demonstrated without using the framework of Nonlinear Normal Modes and the complexification-averaging method. In the context of noise reduction, a TET has been employed in designing a vibroacoustic NES where the essential stiffness nonlinearities (nonlinearizable) have been experimentally implemented with a thin viscoelastic membrane which simulates a cubic nonlinearity (Bellet et al., 2010).

TET has been studied extensively in deterministic frameworks. However, very few studies have been devoted to analyse TET in stochastic cases (Schmidt and Lamarque, 2009; Sapsis et al., 2010). In this paper, uncertainties are taken into account to discuss the robustness of energy pumping. Some parameters of the model considered are taken as uncertain, random variables are associated to it and corresponding probability density functions constructed.

This paper is organized as follows: Section 2 presents the deterministic model which will be used to study the energy pumping phenomenon. Section 3 presents the parameters which will be considered uncertain and the methodology applied to perform a stochastic analysis related to the robustness of the energy pumping. Finally, in Sec. 4 conclusions are outlined.

## 2 THE DETERMINISTIC MODEL USED

The system used to illustrate the energy pumping phenomenon and to discuss its robustness, taking into account uncertainties, has two-degrees-of-freedom, which sketch is shown in Fig. 1.

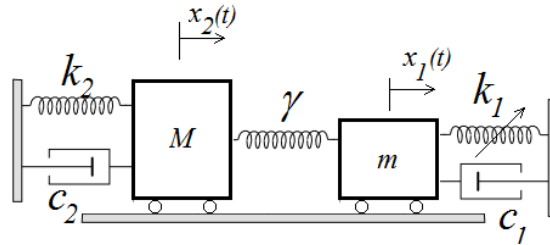


Figure 1: Energy pumping model.

The system is composed of two subsystems (each one is a weak damped oscillator), weakly coupled by a linear stiffness. The first subsystem corresponding to the linear part (or primary system) is composed of the mass  $M$ , the linear spring  $k_2$  and the linear damping  $c_2$ . The second subsystem corresponding to the NES is composed of the mass  $m$ , the cubic spring  $k_1$  and the linear damping  $c_1$ . A weak linear spring  $\gamma$  couples the two subsystems. This configuration is referred as the grounded configuration because the NES is connected to the ground. The equations of motion are given by Eq.1:

$$\begin{cases} m\ddot{x}_1 + c_1\dot{x}_1 + k_1x_1^3 + \gamma(x_1 - x_2) = 0 \\ M\ddot{x}_2 + c_2\dot{x}_2 + k_2x_2 + \gamma(x_2 - x_1) = 0 \end{cases} \quad (1)$$

where  $x_1(t)$  and  $x_2(t)$  denote the displacements of the NES and the primary system, respectively.

The simulations will be performed considering the following values for the systems parameters:  $M = 1 \text{ kg}$ ,  $m = 0.1 \text{ kg}$ ,  $k_2 = 0.9 \text{ N/m}$ ,  $k_1 = 0.1 \text{ N/m}$ ,  $c_1 = 0.01 \text{ Ns/m}$ ,  $c_2 = 0.05 \text{ Ns/m}$  and  $\gamma = 0.05 \text{ N/m}$ . Only free responses associated to impulsive excitation of the primary system will be analyzed, which corresponds to the following initial conditions:  $x_1 = 0$ ,  $x_2 = 0$ ,  $\dot{x}_1 = 0$  and  $\dot{x}_2 = \sqrt{2h}$ , where  $h$  corresponds to the initial energy given to the system.

In order to discuss the energy pumping effectiveness, two different values of  $\gamma$  will be considered.

## 2.1 First case: $\gamma = 0$ - uncoupled systems

The first case to be considered is when the systems are uncoupled, i.e.,  $\gamma = 0$ . Figure 2 shows the displacement of the mass  $M$ , under the initial energy  $h = 0.15$  J.

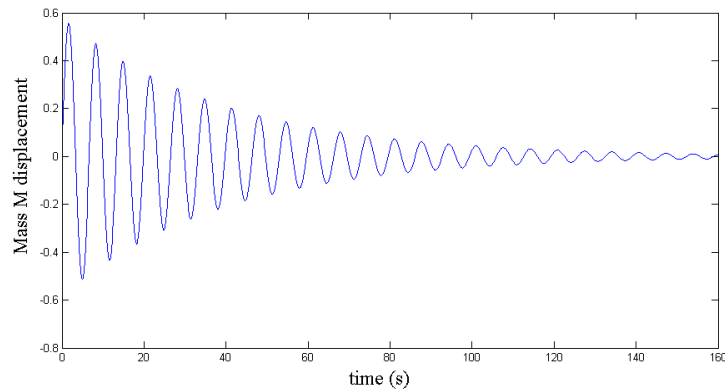


Figure 2: Displacement of the mass  $M$  for the uncoupling case  $\gamma = 0$ .

Clearly, the mass  $m$  is at rest and the displacement of  $M$  decreases exponentially with the time, as expected for a single mass-spring-damper system.

## 2.2 Second case: $\gamma = 0.05$

The second case is one wherein the subsystems are coupled, setting  $\gamma = 0.05$ . In order to illustrate the role of the parameters in energy pumping, three cases are considered, changing the numerical values for the initial energy  $h$  ( $h = 0.01$ ,  $h = 0.05$  and  $h = 1.125$ ). The results are shown in Fig. 3:

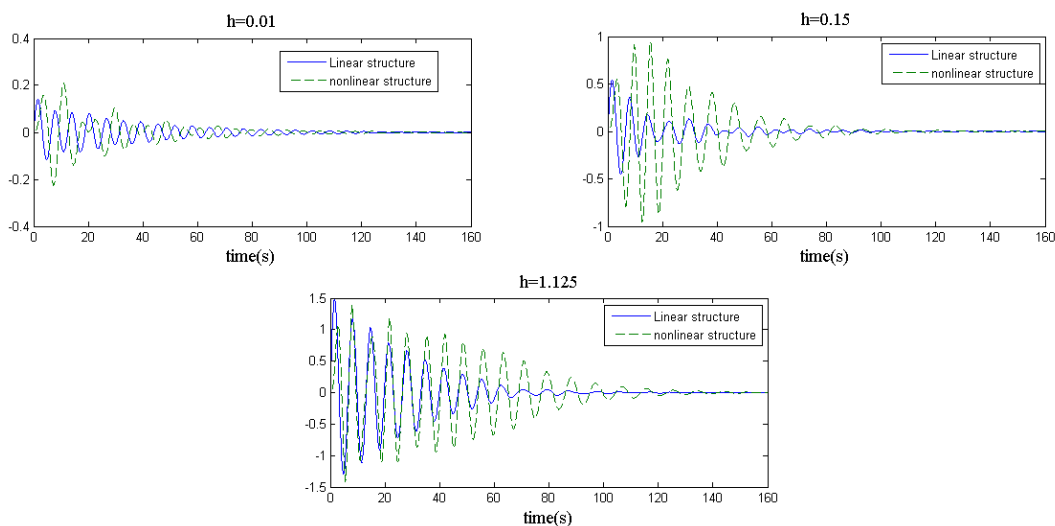


Figure 3: Displacements of the linear structure (mass  $M$ ) and nonlinear structure (mass  $m$ ), for different values of  $h$ .

The energy pumping is more effective for  $h = 0.15$ . For  $h = 0.01$  it does not happen, and for  $h = 1.125$  it is less present, when the displacements of the masses  $M$  and  $m$  are compared with those for  $h = 0.15$ .

In general, when the energy pumping phenomenon happens, the movement can be separated in two phases. In the case presented, one can say that the first phase occurs for  $0 < t < 40$ , when  $h = 0.15$ , and for  $0 < t < 60$ , when  $h = 1.125$ . In this phase, the energy is pumped from the linear oscillator (mass  $M$ ) to the nonlinear oscillator (mass  $m$ ), in a unique and irreversible way, up to an oscillation amplitude achieved by the mass  $M$ . Moreover, still in the first phase, the displacements of the two oscillators are almost in-phase, and the NES oscillation amplitude is large. During the second phase ( $40 < t$ , for  $h = 0.15$  and  $60 < t$ , for  $h = 1.125$ ), the two oscillators dissipate energy, because the mass  $m$  stores a large part of the energy. In addition, the displacements of the two oscillators are almost out-of-phase. This suggests that an internal resonance between the linear oscillator and the nonlinear oscillator plays an important role, during the energy pumping phase.

It is also important to note that the energy pumping happens more effectively when  $h = 0.15$ . Even with values greater than this, the energy pumping is not as effective. One can say that there is an optimum value for  $h$  such that the energy pumping is maximum.

Another interesting way to identify the energy pumping can be observed by computing the energies corresponding to the primary system and to the NES. For the primary system (the linear subsystem), the total energy ( $EL$ ) is given by Eq.2:

$$EL = 0.5 * M * \dot{y}_2^2 + 0.5 * \gamma * (y_2 - y_1)^2 + 0.5 * k_2 * y_2^2 \quad (2)$$

and considering the NES (the nonlinear subsystem), the total energy ( $ENL$ ) is given by

$$ENL = 0.5 * m * \dot{y}_1^2 + 0.5 * \gamma * (y_1 - y_2)^2 + 0.5 * k_1 * y_1^2. \quad (3)$$

We again consider three cases:  $h = 0.01$ ,  $h = 0.15$  and  $h = 1.125$ . The total energy stored in the nonlinear oscillator  $ENL$  and the total energy stored in the linear oscillator  $EL$  are shown in Figs. 4 and 5, respectively.

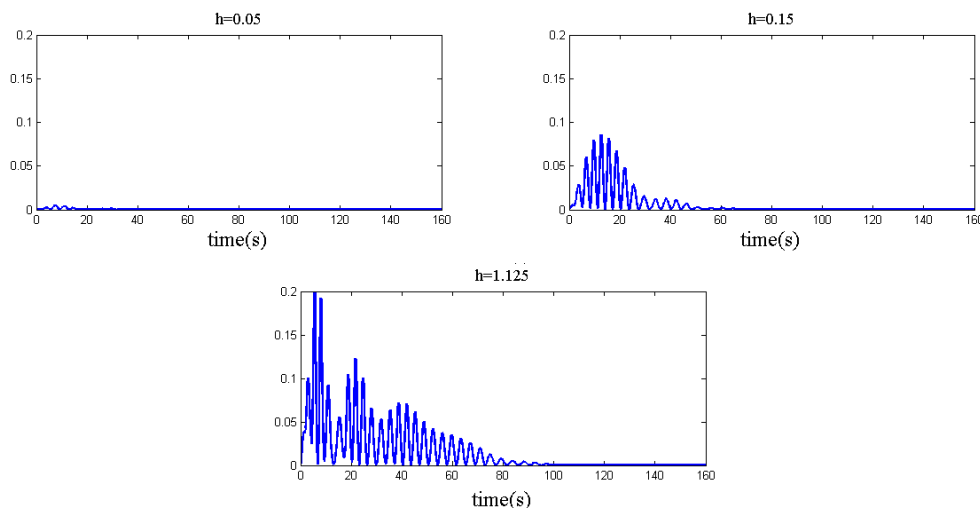


Figure 4: Numerical simulations of energy pumping for different values of  $h$ , considering the energy stored in the nonlinear oscillator (ENL).

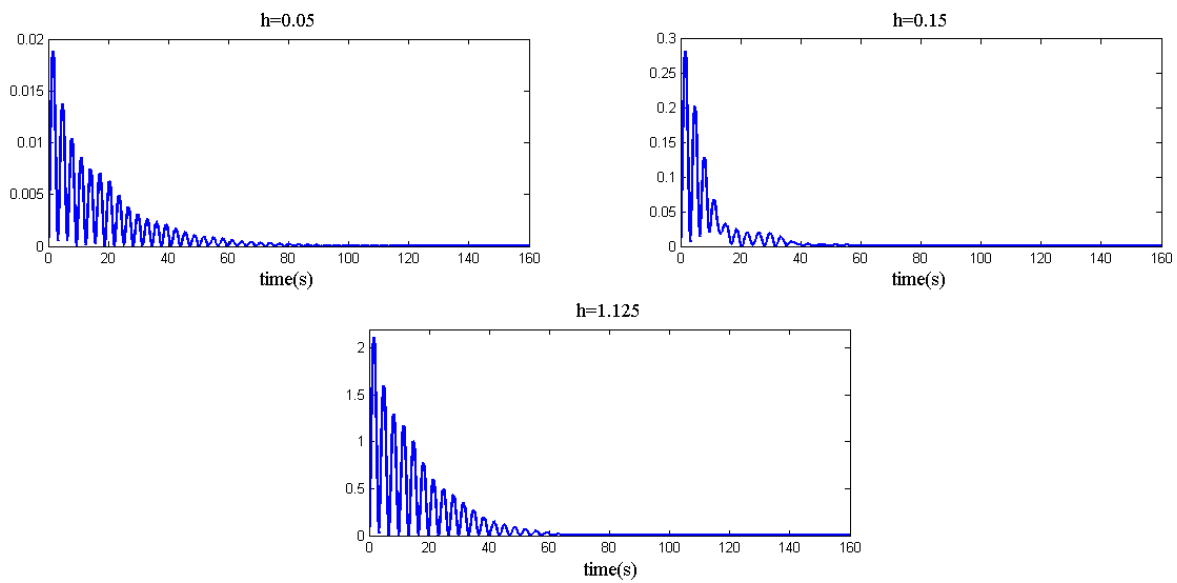


Figure 5: Numerical simulations of energy pumping for different values of  $h$ , considering the energy stored in the linear oscillator (EL).

From the graphs, it can be noted that the energy pumping can be better observed for  $h = 0.15$ . Note that the y-axis scales are the same for all plots.

However, the energy pumping effect can also be noted if variations on other parameters are considered and not only in  $h$ . For example, the coupling stiffness ( $\gamma$ ) has an important role in this process. In order to illustrate this comment,  $h$  is maintained at 0.15 and different values of  $\gamma$  are considered. The results are shown in Fig. 6.

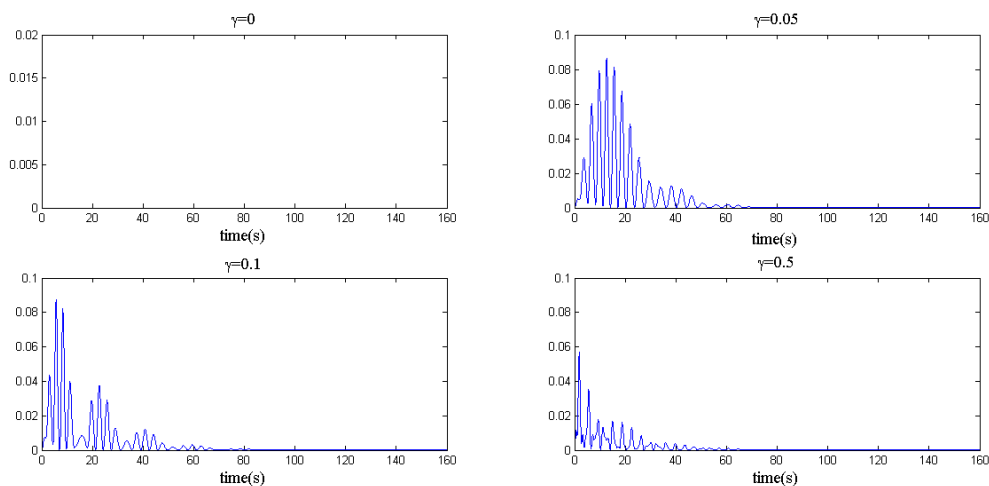


Figure 6: Numerical simulations of energy pumping for different values of  $\gamma$ , considering the energy stored in the nonlinear oscillator.

For  $\gamma = 0.05$ , the energy pumping is well effective, but when  $\gamma = 0.5$ , the phenomenon disappears.

Thus, verifying the robustness of energy pumping, taking account the uncertainties in some

parameters, seems to be a good idea.

### 3 ENERGY PUMPING ROBUSTNESS

#### 3.1 General considerations

The effects of the nonlinear system, which absorbs the energy, will be analyzed by introducing uncertainties on the  $\gamma$  parameter in order to verify the robustness of the energy transfer, when the parameters values are not well known. It is possible that the energy is absorbed from the linear system through the nonlinear system, weakly coupled to the linear system. Herein, the coupling stiffness is one parameter considered uncertain and the damping related to the linear system is another, because it plays an important role and it is difficult to know its value exactly.

The energy pumping phenomenon happens due to a resonance 1:1 (the two structures oscillate at the same frequency). When the energy pumping happens, a resonance state is produced between the nonlinear oscillator with one linear mode and the energy is transferred to the nonlinear system in a irreversible way.

Hence, it is important to know if the energy pumping can be produced even when the parameters are uncertain, in order to apply the theory to real structures, where the nonlinear structure annexed does not reflect perfectly the theoretical conception and the problems related to the nonlinear identification appear.

#### 3.2 Stochastic modeling

Three parameters will be considered as uncertain. They are the coupling stiffness  $\gamma$ , the damping corresponding to the linear subsystem  $c_1$  and the damping corresponding to the nonlinear subsystem  $c_2$ . Random variables will be associated to these parameters and probability density functions constructed to these random variables using the Maximum Entropy Principle, which states that out of all probability density distributions consistent with a given set of available information, the one with the maximum uncertainty (entropy), given by Eq.4, is chosen:

$$S(p_X) = - \int_{-\infty}^{+\infty} p_X(x) \ln(p_X(x)) dx. \quad (4)$$

The goal is to maximize the entropy  $S$  under the constraints defined by some available information on each random variable.

#### 3.3 Stochastic solver for the uncertain system

Let  $X$  be a random variable associated to one of the three parameters  $\gamma$ ,  $c_1$  and  $c_2$ . The stochastic solver used is based on the Monte Carlo method. First,  $N$  independent realizations  $X(\theta)$  of the random variable  $X$  are obtained using the probability density function constructed. For each realization  $X(\theta)$ , the displacements and the velocities of the masses  $M$  and  $m$  are plotted using the following initial conditions:  $x_1 = 0$ ,  $x_2 = 0$ ,  $\dot{x}_1 = 0$ ,  $\dot{x}_2 = \sqrt{2h}$ .

##### 3.3.1 Parameter $\gamma$ chosen as uncertain

The first parameter to be considered as uncertain is the coupling stiffness  $\gamma$ . The random variable  $K$  is associated to this parameter and the following information is considered as available: (1) the support of the probability density function is  $]0, +\infty[$ , (2) the mean value which is known,  $E[K] = \underline{K}$  and (3) the condition  $E\{\ln(K)\} < +\infty$  which implies that zero is a

repulsive value.

The probability density function  $p_K$  has then to verify the following constraint equations (Soize, 2001; Cataldo et al., 2009):

$$\int_{-\infty}^{+\infty} p_K(k) dk = 1 \quad (5)$$

$$\int_{-\infty}^{+\infty} k p_K(k) dk = \underline{K} \quad (6)$$

$$\int_{-\infty}^{+\infty} \ln(K) p_K(k) dk < +\infty \quad (7)$$

Applying the Maximum Entropy Principle yields the following probability density function for  $K$ :

$$p_K(k) = \mathbf{1}_{]0,+\infty[}(k) \frac{1}{\underline{K}} \left( \frac{1}{\delta_K^2} \right)^{\frac{1}{\delta_K^2}} \times \frac{1}{\Gamma(1/\delta_K^2)} \left( \frac{q}{\underline{K}} \right)^{\frac{1}{\delta_K^2}-1} \exp\left(-\frac{k}{\delta_K^2 \underline{K}}\right), \quad (8)$$

where  $\delta_K = \frac{\sigma_K}{\underline{K}}$  is the coefficient of dispersion of the random variable  $K$  such that  $\delta_K < \frac{1}{\sqrt{2}}$  and  $\sigma_K$  is the standard deviation of  $K$ . It can be verified that  $K$  is a second-order random variable and that  $E\{1/K^2\} < +\infty$ .

Fig. 7 shows the results obtained when  $\delta_K = 0.03$ ,  $\underline{K} = 0.05$ ,  $h = 0.15$  and  $N = 50$  realizations.

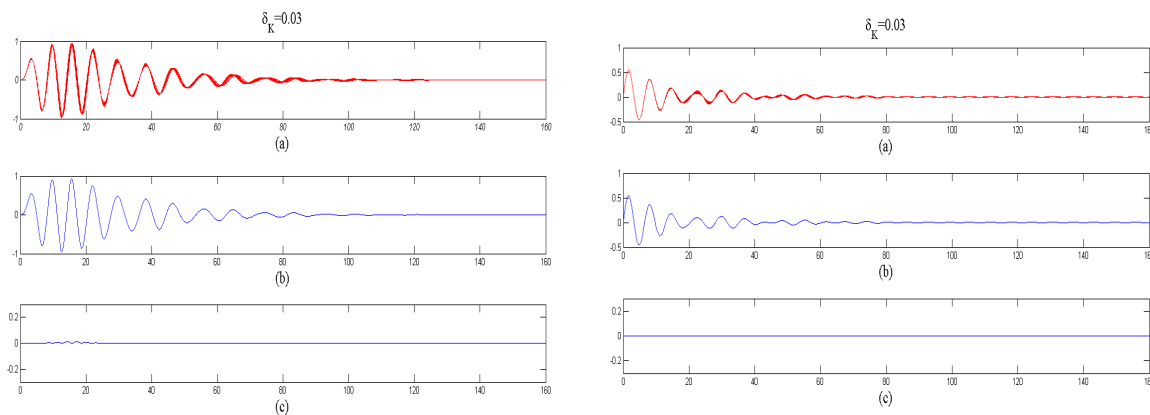


Figure 7: Numerical results for  $\underline{K} = 0.05$  and  $\delta_K = 0.03$ . (a) Realizations of the displacement of the mass. (b) Mean value of the realizations. (c) Standard deviation of the realizations. Left: nonlinear system. Right: linear system.

It can be noted that the energy pumping phenomenon is produced and the energy pumping is effective for all the realizations (see Fig. 7 (top)). The mean values of  $x_1(t)$  and  $x_2(t)$  are characterized by two different behaviors. In the initial phase ( $0 < t < 15$ ), the mean displacements of the two oscillators are almost in-phase, the oscillation amplitude of the mean displacement of the NES is large and the decay of the primary system amplitude is linear and very fast compared with the single mass-spring-damper system (see Fig. 2). This behavior recalls the energy



pumping condition, characterized by an irreversible transfer of energy from the primary system to the nonlinear subsystem (energy localization in the NES), where it is dissipated. In the second phase ( $t > 15$ ), the behavior of the two oscillators is similar to that of the weakly excited case, showing out-of-phase displacements. Note that in this case, the standard deviations of  $x_1(t)$  and  $x_2(t)$  are small.

Fig. 8, Fig. 9 and in Fig. 10 show results obtained increasing the dispersion  $\delta_K$ .

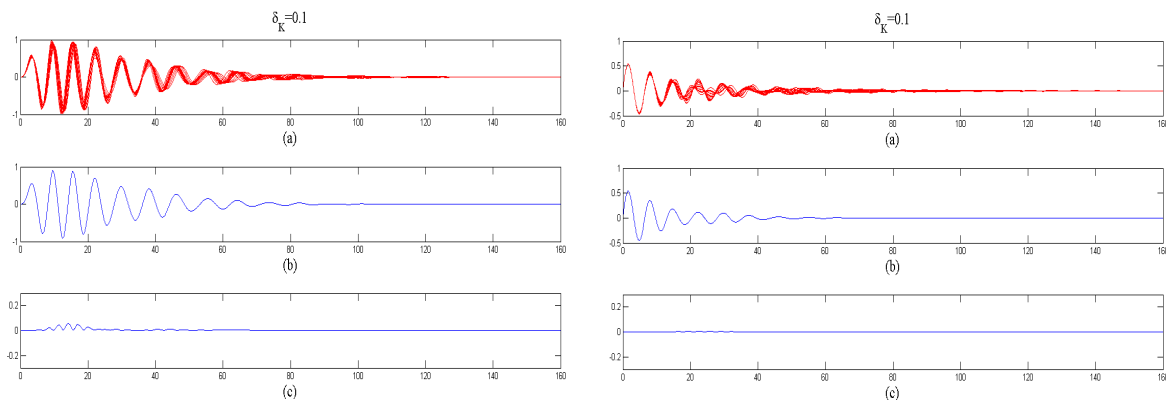


Figure 8: Numerical results for  $\bar{K} = 0.05$  and  $\delta_K = 0.1$ . (a) Realizations of the displacement of the mass. (b) Mean value of the realizations. (c) Standard deviation of the realizations. Left: nonlinear system. Right: linear system.

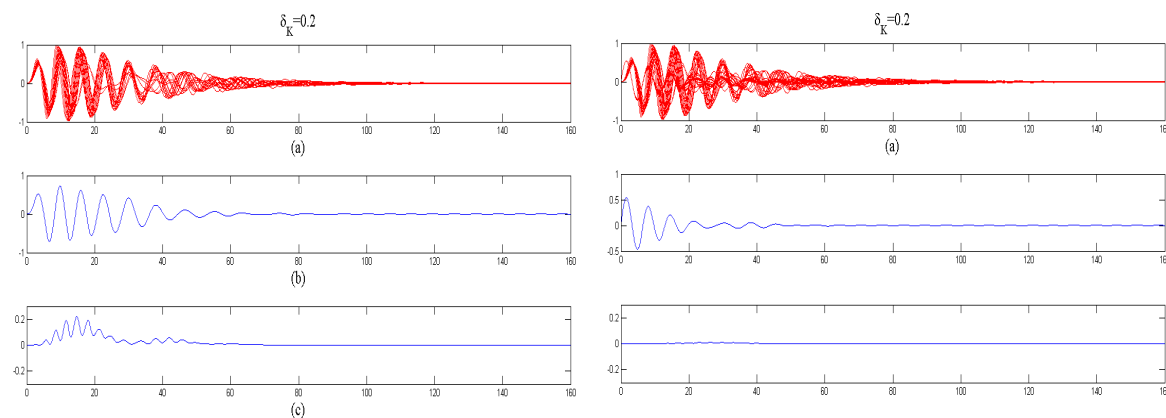


Figure 9: Numerical results for  $\bar{K} = 0.05$  and  $\delta_K = 0.2$ . (a) Realizations of the displacement of the mass. (b) Mean value of the realizations. (c) Standard deviation of the realizations. Left: nonlinear system. Right: linear system.

For  $\delta_K = 0.1$  (see Fig. 8), although the standard deviation is large, the energy pumping still happens. For  $\delta_K = 0.2$  (see Fig. 9), the energy pumping disappears for some realizations, although the mean value still presents the phenomenon. The standard deviation is already more pronounced. However, when  $\delta_K = 0.5$ , the energy pumping disappears for more realizations and, in this case, the mean value of the realizations show that the energy pumping does not exist anymore.

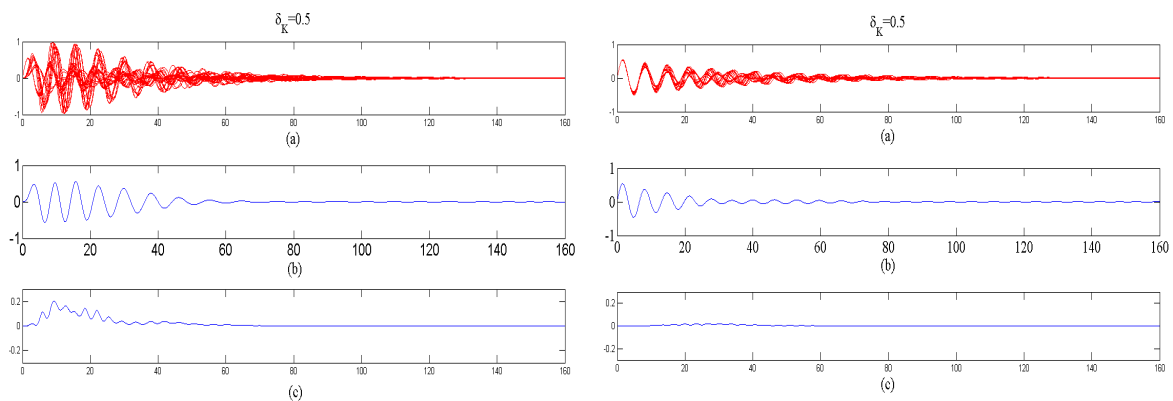


Figure 10: Numerical results for  $\bar{K} = 0.05$  and  $\delta_K = 0.3$ . (a) Realizations of the displacement of the mass. (b) Mean value of the realizations. (c) Standard deviation of the realizations. Left: nonlinear system. Right: linear system.

### 3.3.2 Parameter $c_1$ chosen as uncertain

If we consider the nonlinear damping  $c_1$  as uncertain, a random variable  $C_1$  can be assigned to it. It will be considered the same available information as it was considered for  $K$  and, consequently, using the Maximum Entropy Principle, the probability density function constructed will have the same expression as the one constructed for  $K$ . Using the Monte Carlo Method as well, realizations of the displacements of the nonlinear mass are constructed and the results are shown in Figs. 11 and 12 for two different values of the dispersion coefficient  $\delta_{C_1} = 0.2$  and  $\delta_{C_1} = 0.5$ , respectively.

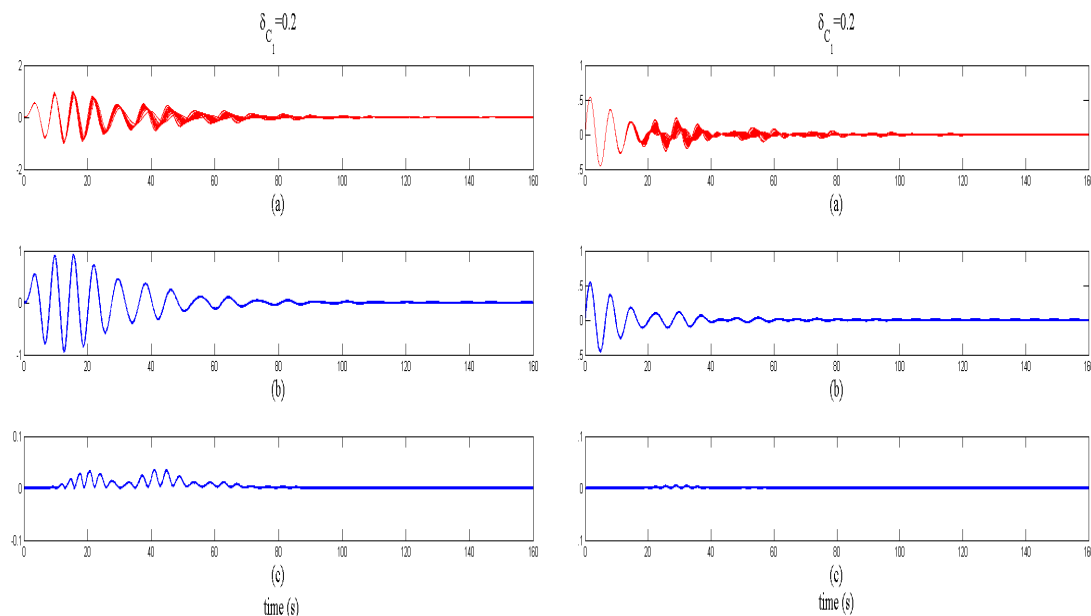


Figure 11: Numerical results for  $\delta_{C_1} = 0.2$ . (a) Realizations of the displacement of the mass  $m$  (nonlinear system). (b) Mean value of the realizations. (c) Standard deviation of the realizations.

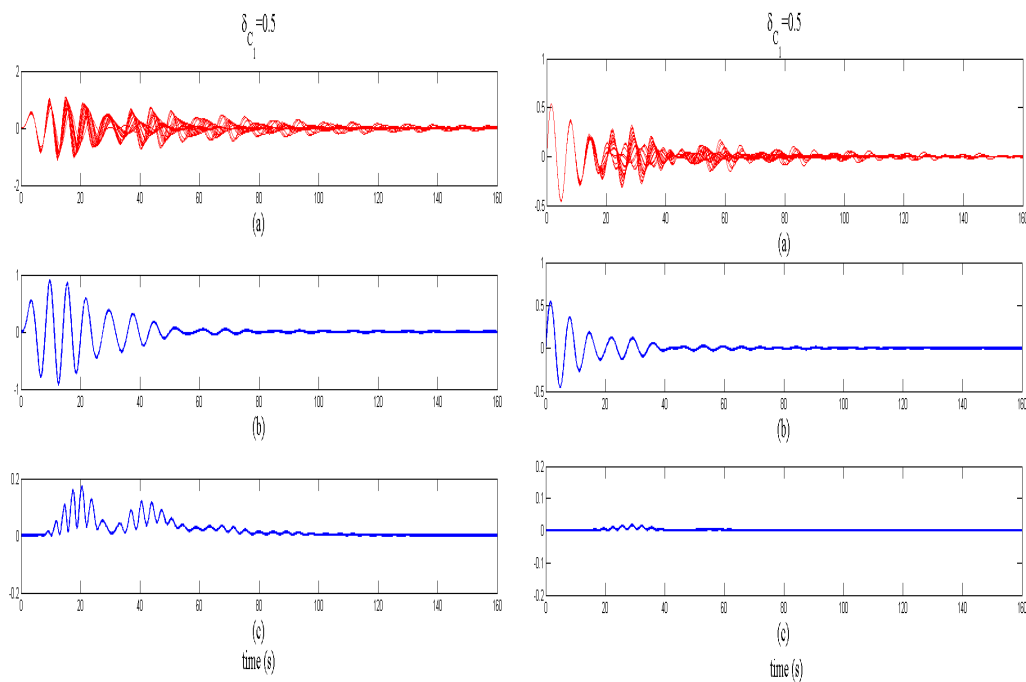


Figure 12: Numerical results for  $\delta_{C_1} = 0.5$ . (a) Realizations of the displacement of the mass  $m$  (nonlinear system). (b) Mean value of the realizations. (c) Standard deviation of the realizations.

It is interesting to note that even when the dispersion is great,  $\delta_K = 0.5$ , the energy pumping takes place. This can be perceived looking at the realizations plots or looking at the mean value plot, although the standard deviation show a large value.

A new trial is performed, now considering  $\delta_{C_1} = 0.7$  and the results are shown in Fig.13.

Even with the dispersion near the maximum value permitted, according to the Maximum Entropy Principle to its probability distribution, the energy pumping takes place. However, it can be noted that the standard deviation is more pronounced in the first phase than in the second phase.

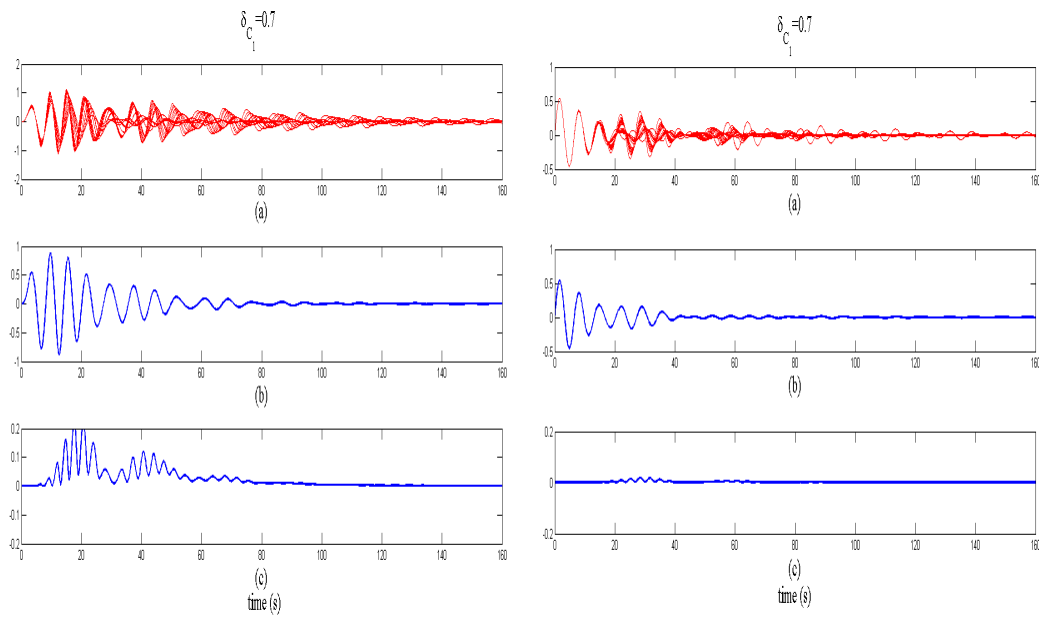


Figure 13: Numerical results for  $\delta_{C_1} = 0.7$ . (a) Realizations of the displacement of the mass  $m$  (nonlinear system). (b) Mean value of the realizations. (c) Standard deviation of the realizations.

### 3.3.3 Parameter $c_2$ chosen as uncertain

Now, the linear damping  $c_2$  is considered as uncertain and the random variable  $C_2$  is assigned to it. The available information is the same as considered for  $C_1$  and, consequently, using the Maximum Entropy Principle, the corresponding probability density function constructed will have the same expression as the one constructed for  $C_2$ . Using the Monte Carlo Method, realizations of the displacements of the linear and the nonlinear masses are shown in Figs. 14 and 15 for  $\delta_{C_2} = 0.2$  and  $\delta_{C_5} = 0.5$ , which are the dispersion coefficients, respectively.

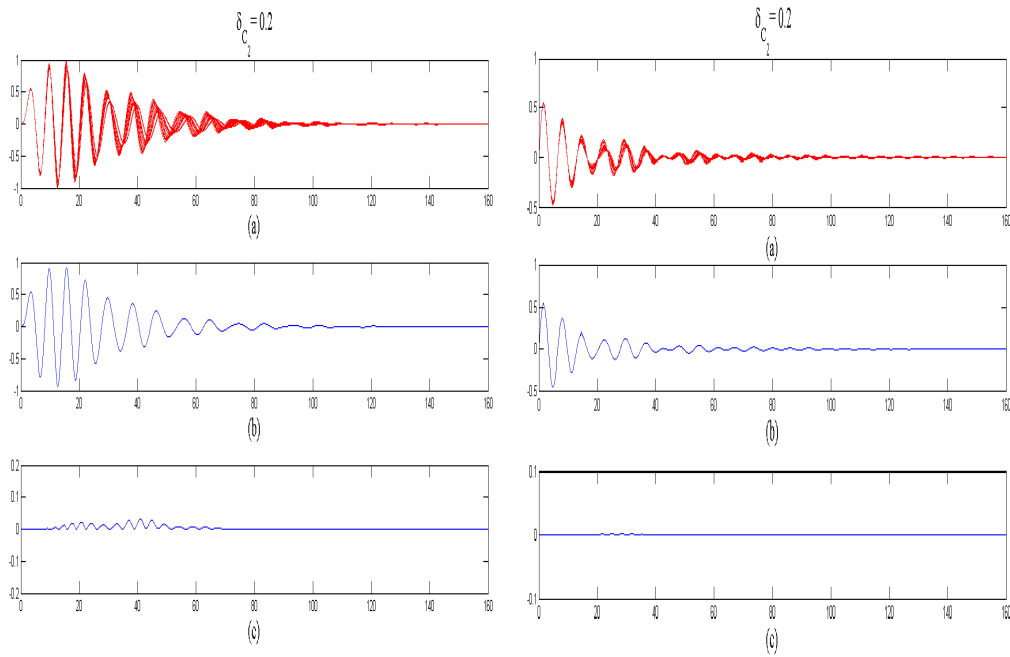


Figure 14: Numerical results for  $\delta_{C_2} = 0.2$ . (a) Realizations of the displacement of the mass  $m$  (nonlinear system). (b) Mean value of the realizations. (c) Standard deviation of the realizations.

It can be noted that the energy pumping takes place in both cases. Something very interesting is that in this case the standard deviation is more pronounced for the second phase, exactly the opposite for when the uncertain parameter  $c_1$  was analyzed. Related to the mean value, the energy pumping takes place.

A greater value for the dispersion coefficient is then considered,  $\delta_{C_2} = 0.7$ . The results are shown in Fig. 16.

The energy pumping still takes place if the mean mean value of the displacements is observed. However, the dispersion of the realizations changes from the first phase to the second one, when the nonlinear part is considered. It shows that the difference between the realizations becomes more important after the first phase.

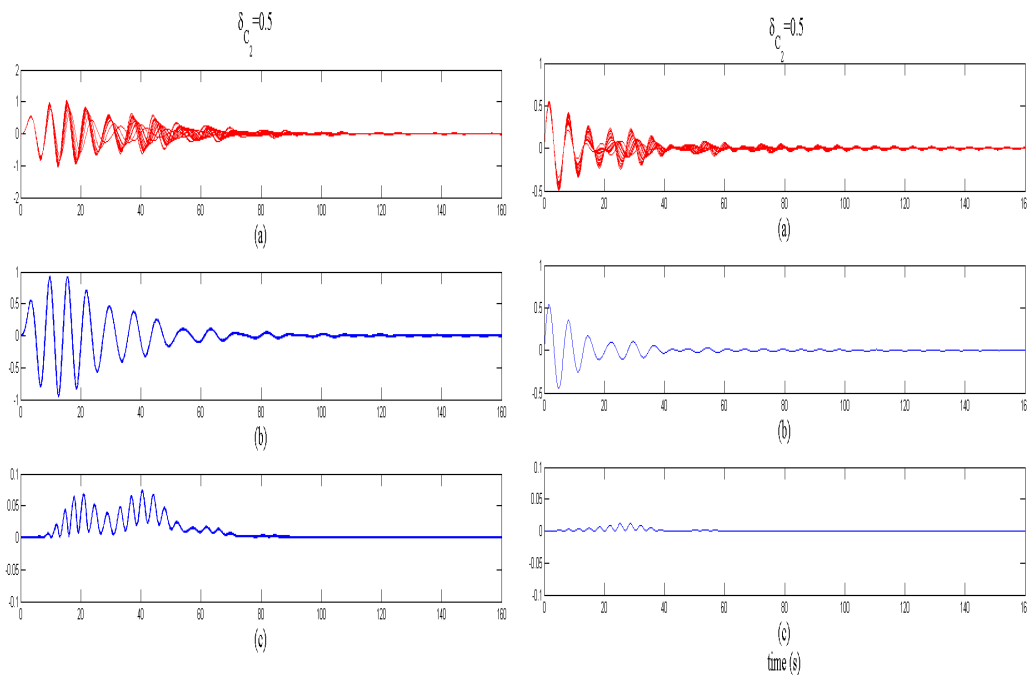


Figure 15: Numerical results for  $\delta_{C_2} = 0.5$ . (a) Realizations of the displacement of the mass  $m$  (nonlinear system). (b) Mean value of the realizations. (c) Standard deviation of the realizations.

#### 4 CONCLUSIONS

This paper analyzes energy pumping using a system composed of two subsystems, one linear and another nonlinear, to discuss the energy pumping phenomenon. The main objective was to take into account uncertainties in some parameters of the system and to analyze the robustness of the energy pumping.

Three parameters were considered as uncertain: the coupling stiffness and the two dampers of the linear and the nonlinear subsystems. Probability density functions were assigned to random variables, related to these parameters.

The main conclusions obtained were that the system is more robust when uncertainties related to the dampers are taken into account, because with a greater level of dispersion in this parameter, the energy pumping phenomenon could still be observed. For the same level of dispersion, the effects of the three random variables were compared and the system results were more sensitive to variations of the random variable associated to the stiffness coupling.

The displacements of the linear subsystem are less sensitive to the variations of the uncertain parameter than the displacements of the nonlinear subsystem.

In addition, it was observed that when the damper of the nonlinear subsystem was considered uncertain, the standard deviation was more pronounced in the first phase and when the damper related to the linear subsystem was considered uncertain, the standard deviation was more pronounced in the second phase. Then, the first phase is more robust for variations in the damper of the nonlinear subsystem and less robust for variations in the damper of the linear subsystem. On the other hand, the second phase is more robust for variations in the damper of the linear subsystem and less robust for variations in the damper of the nonlinear subsystem.

An idea for a future study is to consider other parameters as uncertain and employ other

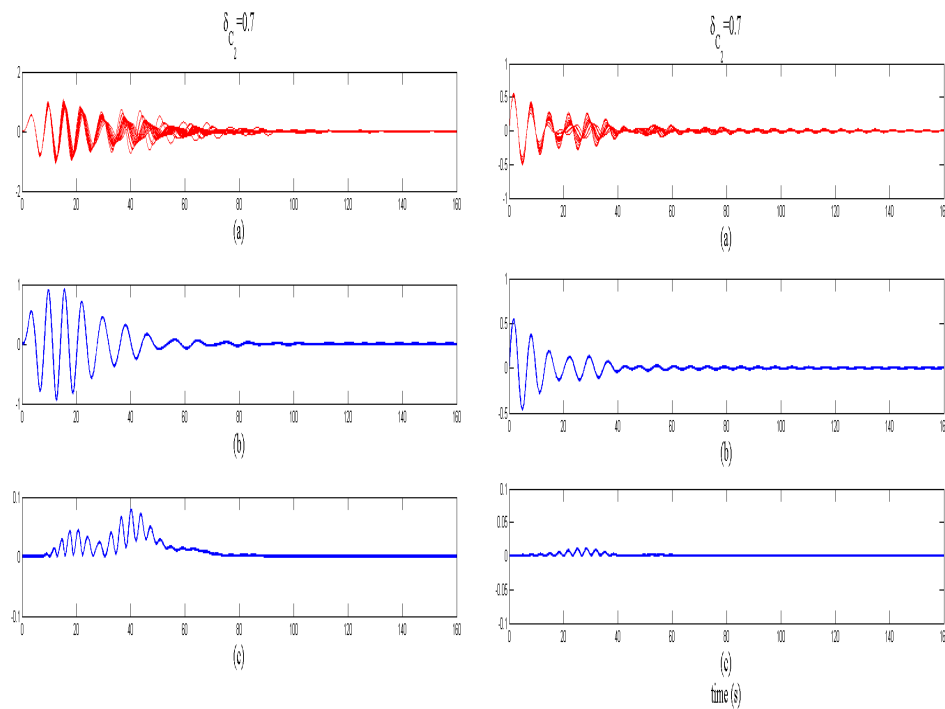


Figure 16: Numerical results for  $\delta_{C_2} = 0.7$ . (a) Realizations of the displacement of the mass  $m$  (nonlinear system). (b) Mean value of the realizations. (c) Standard deviation of the realizations.

methodologies to take it into account. Other quantities can also be analyzed, for example, the energy variation of the system.

## REFERENCES

- Bellet R., Cochelin B., Herzog P., and Mattei P.O. Experimental study of targeted energy transfer from an acoustic system to a nonlinear membrane absorber. *Journal of Sound and Vibration*, 329:2768–2791, 2010.
- Cataldo E. and Soize C., Sampaio R., and Desceliers C. Probabilistic modeling of a nonlinear dynamical system used for producing voice. *Computational Mechanics*, 43:265–275, 2009.
- Ema S. and Marui E. A fundamental study on impact dampers. *Int. J. Mach. Tools Manufact.*, 34:407–421, 1994.
- Gendelman O., Manevitch L., Vakakis A., and M'Closkey R. Energy pumping in nonlinear mechanical oscillators: Part I - Dynamics of the underlying hamiltonian systems. *Journal of Applied Mechanics*, 68:34–41, 2001.
- Gourdon E., Alexander N., Taylor C., Lamarque C., and Pernot S. Nonlinear energy pumping under transient forcing with strongly nonlinear coupling: Theoretical and experimental results. *Journal of Sound and Vibration*, 300:522–551, 2007.
- Jang X., McFarland D., Bergman L., and Vakakis A. Steady state passive nonlinear energy pumping in coupled oscillators: theoretical and experimental results. *Nonlinear Dynamics*, 33:87–102, 2003.
- Nucera F., Lo Iacono F., McFarland D., Bergman L., and Vakakis A. Application of broadband nonlinear targeted energy transfers for seismic mitigation of a shear frame: Experimental results. *Journal of Sound and Vibration*, 313:57–76, 2008.
- Sapsis T., Vakakis A., and Bergman L. Effect of stochasticity on targeted energy transfer from a linear medium to a strongly nonlinear attachment. *Probabilistic Engineering Mechanics*, 2010.
- Schmidt F. and Lamarque C.H. Computation of the solutions of the fokker-Planck equation for one and two dof systems. *Communications in Nonlinear Science and Numerical Simulation*, 14:529–542, 2009.
- Soize C. Maximum entropy approach for modeling random uncertainties in transient elastodynamics. *J. Acoust. Soc. Am.*, 109:1979–1996, 2001.
- Vakakis A. and Gendelman O. Energy pumping in nonlinear mechanical oscillators: Part II - Resonance capture. *Journal of Applied Mechanics*, 68:42–48, 2001.
- Vakakis A., Gendelman O., Bergman L., McFarland D., Kerschen G., and Lee Y. *Nonlinear targeted energy transfer in mechanical and structural systems*, volume 156 of *Solid mechanics and its applications*. Springer, 2008.

## 5 ACKNOWLEDGMENTS

This work was supported by FAPERJ (Fundação de Amparo à Pesquisa no Rio de Janeiro - programa Jovens Cientista do Nosso Estado), by CAPES (CAPES/COFECUB project N. 672/10) and by CNPq (Brazilian Agency Conselho Nacional de Desenvolvimento Científico e Tecnológico).